

Spectrum Sensing in Wideband OFDM Cognitive Radios

Chien-Hwa Hwang* and Shih-Chang Chen†
 chhwang@ee.nthu.edu.tw* and g945606@oz.nthu.edu.tw†
 Institute of Communications Engineering,
 National Tsing Hua University,
 Hsinchu, Taiwan.

Abstract

In this paper, detection of the primary user (PU) signal in an orthogonal frequency division multiplexing (OFDM) based cognitive radio (CR) system is addressed. According to the prior knowledge of the PU signal, three detection algorithms based on the Neyman-Pearson philosophy are proposed. In the first case, a Gaussian PU signal with completely known probability density function (PDF) except for its received power is considered. The frequency band that the PU signal resides is also assumed known. Detection is performed individually at each OFDM sub-carrier possibly interfered by the PU signal, and the results are then combined to form a final decision. In the second case, the sub-carriers that the PU signal resides are known. Observations from all possibly interfered sub-carriers are considered jointly to exploit the fact that the presence of a PU signal interferes all of them simultaneously. In the last case, it is assumed no PU signal prior knowledge is available. The detection is involved with a search of the interfered band. The proposed detector is able to detect an abrupt power change when tracing along the frequency axis.

I. INTRODUCTION

Radio spectrum is the medium for all types of wireless communications, such as cellular phones, satellite-based services, wireless low-powered consumer devices, and so on. Since most of the usable spectrum has been allocated to existing services, the radio spectrum has become a precious and scarce resource, and there is an urgent concern about the availability of spectrum for future needs. Nonetheless, the allocated radio spectrum today is not efficiently utilized. According to a report of the United States Federal Communications Commission (FCC) [1], there are large temporal and geographic variations in the utilization of allocated spectrum ranging from 15% to 85%. Moreover, according to Defense Advanced Research Projects Agency (DARPA), in the United States, only 2% of the spectrum is in use at any moment. It is then clear that the solution to the spectrum scarcity problem is dynamically looking for the spectrum "white spaces" and using them opportunistically. Cognitive radio (CR) technology, defined first by J. Mitola [2], [3], is thus advocated by FCC as a candidate for implementing opportunistic spectrum sharing. The spectrum management rule of CR is that all new users for the spectrum are secondary (cognitive) users and requiring that they must detect and avoid the primary user.

To achieve the goal of CR, it is a fundamental requirement that the cognitive user performs spectrum sensing to detect the presence of the primary user (PU) signal. Digital signal processing techniques can be employed to promote the sensitivity of the PU signal sensing. Three commonly adopted methods are matched filtering, energy detection [4]–[10], and PU signal feature detection with the cyclo-stationary feature most widely adopted [11]–[14]. Moreover, cooperation among cognitive users in spectrum sensing can not only reduce the detection time and thus increase the agility, but also alleviate the problem that a cognitive user fails to detect the PU signal because it is located at a weak-signal region [8]–[10], [15]–[20]. For overview of these approaches and their properties, see [21]–[23].

It is concluded in [24] that orthogonal frequency division multiplexing (OFDM) is the best physical layer candidate for a CR system since it allows easy generation of spectral signal waveforms that can fit into discontinuous and arbitrary-sized spectrum segments. Besides, OFDM is optimal from the viewpoint of capacity as it allows achieving

¹Chien-Hwa Hwang is the author for correspondence.

the Shannon channel capacity in a fragmented spectrum. Owing to these reasons, in this paper, we conduct spectrum sensing in an OFDM based CR system.

In detection theory, the Neyman-Pearson (NP) criterion is used when there is difficulty in determining the prior probabilities and assigning costs [25], which is the case in our PU signal detection. The NP detector compares the likelihood ratio (LR) with a threshold determined by the constraint of false alarm probability to decide which hypothesis is true. However, in many cases, some PU signal parameters, such as power level, correlation properties, frequency band, and so on, may not be known. At this time, the PU signal detection problem becomes a composite hypothesis testing, which requires performing estimation for those unknown parameters in the probability density function (PDF) of the observation for either hypothesis. Thus, the degree of detector complexity is directly related to our knowledge of the signal and noise characteristics in terms of their PDFs. Moreover, since the estimation error is not negligible, the detection performance decreases as we have less specific knowledge of the signal and noise characteristics. According to the prior knowledge about the PU signal, three cases of PU signal detection in a cognitive OFDM system are considered in this paper.

In Case A, we consider a Gaussian PU signal of known frequency band and with only the average received power in its PDF being unknown. The normalized covariance matrix of the PU signal, i.e. unity diagonal elements, can be derived directly from the model assumed for it. As the normalized covariance matrix of the PU signal received at each OFDM sub-carrier is distinct, PU signal detection for this case is executed individually at each sub-carrier, and the results are then combined together to form a final decision. In Case B, neither the model of the PU signal nor its distribution is known to the detector. The only thing known is the frequency band that the PU signal resides. The band is assumed to be a continuous segment of sub-carriers. To incorporate the fact that, once a PU signal occurs, several sub-carriers in a row are interfered simultaneously, the detector makes its decision by jointly considering observations from all possibly interfered sub-carriers. In Case C, no prior knowledge of the PU signal is available. Thus, the detection is involved with a search of possibly interfered band. The proposed detector is able to detect an abrupt power change when tracing along sub-carriers.

The organization of this paper is summarized as follows. In Section II, the signal model of a cognitive OFDM system interfered by a PU signal is derived, and the three cases concerning the PU signal prior knowledge are also described. In Section III, the design of PU signal detectors under three cases of PU signal prior information mentioned in Section II are carried out. Simulation results of the proposed detection algorithms are given in Section IV. Finally, we conclude this paper in Section V.

II. PU SIGNAL DETECTION IN A COGNITIVE OFDM SYSTEM

Consider a wideband cognitive OFDM system with Q sub-carriers. The binary data stream generated from the source is encoded and interleaved, and then subdivided into groups of B bits used to generate blocks of Q symbols, where each symbol assumes one of L possible values with $B = Q \log_2 L$. It is assumed that $(\log_2 L)$ -ary phase shift keying (PSK) modulation is employed. We denote the constellation points corresponding to the n -th block of Q symbols by $\mathcal{S}(n) = \{S_0(n), S_1(n), \dots, S_{Q-1}(n)\}$. The n -th OFDM symbol is generated by feeding $\mathcal{S}(n)$ into a Q -point inverse discrete Fourier transform (IDFT) and pre-appending the output with cyclic prefix (CP). The resultant signal is up-converted to the carrier frequency, and then transmitted over a wireless fading channel.

At the receiver, after the frequency down conversion and the CP removal, the output signal is passed through a Q -point discrete Fourier transform (DFT). In the presence of a PU signal, the DFT output corresponding to the n -th OFDM symbol is given by

$$Y_q(n) = H_q(n) \cdot S_q(n) + I_q(n) + W_q(n), \quad 0 \leq q \leq Q - 1, \quad (1)$$

where $H_q(n)$ is the frequency response of the channel at sub-carrier q experienced by the n -th OFDM symbol, and $\{I_q(n)\}$ and $\{W_q(n)\}$ are the contributions resulting from the PU signal and additive white Gaussian noise (AWGN), respectively.

Suppose that a PU signal occupies the frequency band extending from the q_0 -th to the q_1 -th sub-carriers of the OFDM system. If the information of the PU signal frequency band, i.e. q_0 and q_1 , is known to the detector, the detection algorithm decides whether the signal $\{I_q(n)\}$ is present in (1) based on the observation $\{Y_q(n) : 0 \leq n \leq N - 1, q_0 \leq q \leq q_1\}$, where N is the observation length at each sub-carrier, and, if any, the prior knowledge of the PU signal. When q_0 and q_1 are not known, the observation $\{Y_q(n)\}$ needs to be extended to all sub-carriers $0 \leq q \leq Q - 1$.

TABLE I lists three cases regarding the amount of prior knowledge about the PU signal, including the received power, the signal model, probability distribution, and the frequency band it resides. In all three cases, the received power of the PU signal is unknown. In Case A, it is assumed that the sub-carrier indices $[q_0, q_1]$ occupied by the PU signal are known, the stochastic process $\{I_q(n)\}$ observed at each sub-carrier $q_0 \leq q \leq q_1$ is Gaussian, and the $N \times N$ normalized covariance matrices \mathbf{C}_q 's of the random signal $\{I_q(n)\}_{n=0}^{N-1}$ at $q_0 \leq q \leq q_1$ can be obtained from the PU signal model. The normalization factor to obtain \mathbf{C}_q is the PU signal received power at that sub-carrier, and \mathbf{C}_q has diagonal components equal to one. In Case B, the assumptions of known PU signal model and Gaussian distribution are removed. It will be clear this case serves as an intermediate stage for developing the detector in Case C, where no prior PU signal knowledge is available.

III. DESIGN OF PU SIGNAL DETECTOR

A. Case A: Known PU Signal Model, Probability Distribution, and Frequency Band

Two PU signal models, i.e. a sum of tonal signals and an auto-regressive (AR) stochastic process, are assumed for the detection problem. The PU signal $\{I_q(n)\}_{n=0}^{N-1}$ seen at the q -th OFDM sub-carrier has a covariance matrix $P_I(q)\mathbf{C}_q$, where $P_I(q)$ is the unknown received power of the PU signal at sub-carrier q , and \mathbf{C}_q is the normalized covariance matrix with unit diagonal elements.

1) *Tonal PU Signal*: Here we model the PU signal as the sum of a number of complex sinusoids. Examples include WiMAX and WLAN systems, which also employ OFDM technologies. With this model, the received PU signal is $i(t) = \sum_{l=-\infty}^{\infty} i_l(t - lT_i)^1$, where T_i is the symbol duration, and $i_l(t)$ is the signal containing the l -th symbol. We have

$$i_l(t) = \sum_{k=0}^{K-1} \Re\{d_{l,k}(t)e^{j(2\pi f_i t + \phi)}\}, \quad 0 \leq t \leq T_i, \quad (2)$$

where K , f_i and ϕ are the number of complex sinusoids, the carrier frequency, and the random carrier phase, respectively, $\Re\{\cdot\}$ denotes the real part, and $d_{l,k}(t)$ is the complex baseband signal of the k -th sinusoid. We have

$$d_{l,k}(t) = \zeta_l \cdot X_{l,k} e^{j2\pi kt/T_i}, \quad 0 \leq t \leq T_i,$$

where $X_{l,k}$ is the PSK modulated data of the k -th sinusoid at the l -th symbol, and ζ_l is the channel fading coefficient when symbol l of the PU signal is received. Note that here we assume the fading coefficient is roughly the same for all sinusoids.

Let $\eta = \lfloor T_i/T_s \rfloor$ with T_s the symbol duration of the cognitive OFDM, $\lfloor x \rfloor$ the largest integer no greater than x , and $\beta_{k,q} = [(f_i - f_s + k/T_i)T_s - q]/Q$. It is shown in Appendix I-A that, the (n, m) -th element of the normalized covariance matrix $\mathbf{C}_q(n, m)$ of $\{I_q(n)\}_{n=0}^{N-1}$ is given by

$$\mathbf{C}_q(n, m) = \begin{cases} \left(1 - \frac{|n-m|}{\eta}\right) \frac{\sum_{k=0}^{K-1} e^{j2\pi(n-m)T_s(f_i + k/T_i)} \frac{\sin^2(\pi\beta_{k,q}Q)}{\sin^2(\pi\beta_{k,q})}}{\sum_{k=0}^{K-1} \frac{\sin^2(\pi\beta_{k,q}Q)}{\sin^2(\pi\beta_{k,q})}}, & |n-m| \leq \eta - 1, \\ 0, & \text{otherwise.} \end{cases} \quad (3)$$

Note that, without the assumption that the fading coefficient ζ_l is roughly the same for all sinusoids, the expression of elements of \mathbf{C}_q given in (3) cannot be obtained.

2) *AR PU Signal*: We consider the time-domain discrete-time PU signal $\{i_p\}$ at the output of the sampler following the frequency down-converter. Suppose that $\{i_p\}$ can be modeled as an r -th order AR random process of

$$i_p = -\sum_{j=1}^r \phi_j i_{p-j} + e_p, \quad (4)$$

¹Here $i(t)$ is the time-domain PU signal, whereas $\{I_q(n)\}$ given in (1) is a frequency-domain signal.

where $\{e_p\}$ is a white Gaussian random sequence with variance ν^2 , and parameters $\{\phi_j\}_{j=1}^r$ are obtained when $\{i_p\}$ has unit power. The contribution of the PU signal at the q -th DFT output for N OFDM symbols is $\mathbf{I}_q = [I_q(0), I_q(1), \dots, I_q(N-1)]^T$, given by

$$\mathbf{I}_q = \mathbf{F}_q \mathbf{i}, \quad (5)$$

where $\mathbf{F}_q = \text{diag}\{\underbrace{\mathbf{f}_q, \mathbf{f}_q, \dots, \mathbf{f}_q}_{N \text{ times}}\}$ with $\mathbf{f}_q = [e^{-j2\pi q \cdot 0/Q} \ e^{-j2\pi q \cdot 1/Q} \ \dots \ e^{-j2\pi q(Q-1)/Q}]$, and $\mathbf{i} = [i_0, i_1, \dots, i_{Q-N-1}]^T$.

It is readily seen that \mathbf{I}_q forms a Gaussian random process as $\{e_p\}$ is modeled to be Gaussian. In Appendix I-B, we show how the normalized covariance matrix \mathbf{C}_q of \mathbf{I}_q given in (5) can be computed.

It is seen that, for the two PU signal models presented above, the normalized covariance matrix \mathbf{C}_q at each sub-carrier $q \in [q_0, q_1]$ that the PU signal resides are distinct. To employ \mathbf{C}_q for PU signal detection, the detection is performed individually at each sub-carrier, and the final decision is made by combining the individual decisions at sub-carriers. In specific, to design a detector based on the Neyman-Pearson philosophy, the detection threshold γ_q at sub-carrier q is determined by a given overall (i.e., combined from all sub-carriers) false alarm probability $P_{\text{FA}} = \alpha$ such that the overall detection probability P_{D} is maximized. Let the decisions made at individual sub-carriers be combined by an OR operation, i.e., the detector decides \mathcal{H}_1 if any of the sub-carriers declares a PU signal is present. For both P_{FA} and P_{D} , we have

$$P_S = 1 - \prod_{q \in [q_0, q_1]} (1 - P_S(q)), \quad S \in \{\text{FA}, \text{D}\}, \quad (6)$$

where $P_S(q)$ is the detection or false alarm probability at sub-carrier q . Letting $P_{\text{FA}}(q)$ equal for all q 's, we obtain the false alarm constraint at each sub-carrier as

$$P_{\text{FA}}(q) = 1 - (1 - \alpha)^{1/B_{\text{PU}}}, \quad (7)$$

where we define the bandwidth of the PU signal as $B_{\text{PU}} = q_1 - q_0 + 1$.

Suppose that the detection is performed when the cognitive OFDM system is not transmitting signals. The hypothesis testing at the q -th sub-carrier is

$$\begin{aligned} \mathcal{H}_0 : Y_q(n) &= W_q(n), \\ \mathcal{H}_1 : Y_q(n) &= I_q(n) + W_q(n), \end{aligned} \quad n = 0, 1, \dots, N-1, \quad (8)$$

where $\{W_q(n)\}$ is complex white Gaussian noise independent of $\{I_q(n)\}$ with distribution $\mathcal{CN}(\mathbf{0}, \sigma_W^2 \mathbf{I})$, and \mathcal{H}_0 and \mathcal{H}_1 represent that the PU signal is off and on, respectively. The PU signal $\{I_q(n)\}_{n=0}^{N-1}$ is given in (33) and (5), respectively, when it is modeled as a sum of tonal signals and an AR random process. Due to the absence of the OFDM signal, $\{Y_q(n)\}$ is a Gaussian random process in either hypothesis.

Since the detection algorithm proposed for this case is done individually at sub-carriers, we omit q in $P_I(q)$ for notational simplicity. The likelihood ratio associated with (8) is

$$L(\mathbf{Y}_q) = \frac{p(\mathbf{Y}_q; P_I, \mathcal{H}_1)}{p(\mathbf{Y}_q; \mathcal{H}_0)}, \quad (9)$$

where $\mathbf{Y}_q = [Y_q(0), Y_q(1), \dots, Y_q(N-1)]^T$, $p(\mathbf{Y}_q; P_I, \mathcal{H}_1)$ is the probability density function (PDF) of \mathbf{Y}_q under \mathcal{H}_1

$$p(\mathbf{Y}_q; P_I, \mathcal{H}_1) = \frac{1}{\pi^N \det(P_I \mathbf{C}_q + \sigma_W^2 \mathbf{I})} \exp\left(-\mathbf{Y}_q^\dagger (P_I \mathbf{C}_q + \sigma_W^2 \mathbf{I})^{-1} \mathbf{Y}_q\right), \quad (10)$$

and $p(\mathbf{Y}_q; \mathcal{H}_0)$ is the PDF under \mathcal{H}_0 obtained by setting P_I in (10) to zero. Using matrix inversion lemma, we have the test statistic $\ln L(\mathbf{Y}_q)$ given as

$$\ln L_G(\mathbf{Y}_q) = \sigma_W^{-2} P_I \mathbf{Y}_q^\dagger \mathbf{C}_q (P_I \mathbf{C}_q + \sigma_W^2 \mathbf{I})^{-1} \mathbf{Y}_q - \ln \det(P_I \mathbf{C}_q + \sigma_W^2 \mathbf{I}). \quad (11)$$

It is seen that the unknown P_I in $(P_I \mathbf{C}_q + \sigma_W^2 \mathbf{I})^{-1}$ cannot be decoupled from the observation \mathbf{Y}_q . Thus, uniformly most powerful (UMP) test does not exist. Consequently, a generalized likelihood ratio test (GLRT) is employed, where P_I in (11) is replaced with its maximum likelihood (ML) estimate \hat{P}_I .

Let \mathbf{C}_q be eigen-decomposed as $\mathbf{C}_q = \mathbf{V}_q \mathbf{\Lambda}_q \mathbf{V}_q^\dagger$, where $\mathbf{V}_q = [\mathbf{v}_{q,0} \ \mathbf{v}_{q,1} \ \cdots \ \mathbf{v}_{q,N-1}]$ and $\mathbf{\Lambda}_q = \text{diag}(\lambda_{q,0}, \lambda_{q,1}, \dots, \lambda_{q,N-1})$. Hence,

$$\det(P_I \mathbf{C}_q + \sigma_W^2 \mathbf{I}) = \prod_{i=0}^{N-1} (P_I \lambda_{q,i} + \sigma_W^2) \quad \text{and} \quad (P_I \mathbf{C}_q + \sigma_W^2 \mathbf{I})^{-1} = \mathbf{V}_q (P_I \mathbf{\Lambda}_q + \sigma_W^2 \mathbf{I})^{-1} \mathbf{V}_q^\dagger$$

The ML estimate of P_I is obtained by substituting the above two relations into $p(\mathbf{Y}_q; P_I, \mathcal{H}_1)$ and finding its maximum. Moreover, we should also note that P_I is non-negative. Thus, we have

$$\hat{P}_I = \max \left(0, \arg \min_P \sum_{i=0}^{N-1} \left(\ln(P \lambda_{q,i} + \sigma_W^2) + \frac{|\mathbf{v}_{q,i}^\dagger \mathbf{Y}_q|^2}{P \lambda_{q,i} + \sigma_W^2} \right) \right). \quad (12)$$

The general solution of the optimization problem involved in (12) is unknown, and numerical methods are normally required. Even if we can solve (12), the statistic distribution of the detector in (11) is intractable, which yields threshold determination of the detector very difficult. Moreover, under \mathcal{H}_0 , the random variable governing the statistics of \hat{P}_I is zero half of the time and Gaussian for the other half. This is in contrast to the usual Gaussian asymptotic statistics of an ML estimate. Thus, the asymptotic chi-squared distribution of GLRT when $N \rightarrow \infty$ does not hold for (11) [26].

Due to the difficulties encountered by GLRT stated in the previous paragraph, we resort to a locally most powerful (LMP) detector [27,28]. We rewrite (8) as $\mathbf{Y}_q \sim \mathcal{CN}(\mathbf{0}, P_I \mathbf{C}_q + \sigma_W^2 \mathbf{I})$ with

$$\mathcal{H}_0 : P_I = 0 \quad \text{versus} \quad \mathcal{H}_1 : P_I > 0.$$

The LMP detector, given by

$$\left. \frac{\partial \ln p(\mathbf{Y}_q; P_I)}{\partial P_I} \right|_{P_I=0} = -\sigma_W^{-2} \text{tr}(\mathbf{C}_q) + \sigma_W^{-4} \mathbf{Y}_q^\dagger \mathbf{C}_q \mathbf{Y}_q, \quad (13)$$

is optimal when P_I is small. Thus, the detector is

$$T_A(\mathbf{Y}_q) = \mathbf{Y}_q^\dagger \mathbf{C}_q \mathbf{Y}_q \underset{\mathcal{H}_0}{\overset{\mathcal{H}_1}{\gtrless}} \gamma_q \quad (14)$$

as the remaining part of (13) can be absorbed into the threshold, where the subscript of $T_A(\cdot)$ indicates it is for Case A. It is seen that LMP has an advantage that no estimate for P_I is needed. An interesting interpretation of LMP detectors as covariance sequence correlators can be found in [28, pp. 80].

Denote by $T_A(\mathbf{Y}_q)|_{\mathcal{H}_i}$ the shorthand for $T_A(\mathbf{Y}_q)$ under \mathcal{H}_i . Under \mathcal{H}_0 , elements of \mathbf{Y}_q are independent, and $T_A(\mathbf{Y}_q)|_{\mathcal{H}_0}$ is a weighted sum of independent chi-squared random variables. No general closed form is known for its distribution [28, pp. 74–75]. Thus, we look for its asymptotic distribution. We have

$$\left. \frac{\partial \ln p(\mathbf{Y}_q; P_I)}{\partial P_I} \right|_{P_I=0} = \sum_{n=0}^{N-1} \left. \frac{\partial \ln p(Y_q(n); P_I)}{\partial P_I} \right|_{P_I=0}, \quad \text{under } \mathcal{H}_0, \quad (15)$$

which by central limit theorem becomes Gaussian. Thus,

$$T_A(\mathbf{Y}_q)|_{\mathcal{H}_0} \overset{a}{\sim} \mathcal{N}(\sigma_W^2 \text{tr}(\mathbf{C}_q), \sigma_W^4 \text{tr}(\mathbf{C}_q^2)), \quad (16)$$

where $\overset{a}{\sim}$ indicates the sense of asymptote, and the formula of

$$\mathbb{E}\{\mathbf{x}^\dagger \mathbf{A} \mathbf{x} \mathbf{x}^\dagger \mathbf{B} \mathbf{x}\} = \text{tr}(\mathbf{A} \mathbf{C}) \text{tr}(\mathbf{B} \mathbf{C}) + \text{tr}(\mathbf{A} \mathbf{C} \mathbf{B} \mathbf{C}) \quad (17)$$

for $\mathbf{x} \sim \mathcal{CN}(\mathbf{0}, \mathbf{C})$ and Hermitian matrices \mathbf{A} and \mathbf{B} [29] is employed. Under \mathcal{H}_1 , due to the PU signal, elements of \mathbf{Y}_q may not be independent. This makes the distribution of $T_A(\mathbf{Y}_q)|_{\mathcal{H}_1}$ difficult to analyze.

To determine the threshold γ_q in (14), we represent the cumulative distribution function (CDF) of $T_A(\mathbf{Y}_q)|_{\mathcal{H}_0}$ as CDF(x). By (7), γ_q is given by

$$\gamma_q = \text{CDF}^{-1}((1 - \alpha)^{1/B_{\text{pu}}}),$$

with an overall false alarm probability α . If N is large enough such that the asymptotic distribution (16) holds, γ_q can be further written as

$$\gamma_q = \sigma_W^2 \text{tr}(\mathbf{C}_q) + \sigma_W^2 \sqrt{\text{tr}(\mathbf{C}_q^2)} \cdot Q^{-1}(1 - (1 - \alpha)^{1/B_{\text{PU}}}),$$

where $Q(x)$ is the Gaussian right-tail probability. On the other hand, if the asymptotic distribution of $T_A(\mathbf{Y}_q)|_{\mathcal{H}_0}$ is not valid, histograms of $T_A(\mathbf{Y}_q)|_{\mathcal{H}_0}$ can be produced by simulations to get an estimate of $\text{CDF}(x)$.

B. Case B: Known PU Signal Frequency Band

In this case, we employ the fact that the PU signal, if present, appears simultaneously at the sub-carriers from q_0 to q_1 . The algorithm developed for this case works for PU signal with the bandwidth $B_{\text{PU}} = q_1 - q_0 + 1 \geq 2$. When $B_{\text{PU}} = 1$, the PU signal can be detected by first estimating its received power and then employing an energy detector [4]–[10].

Unlike in Case A that the detection is performed when the cognitive OFDM is not transmitting signals, the detection method presented for Case B can work when the signal of the cognitive system is present. The OFDM system signalling for the detection algorithm in Case B is illustrated in Fig. 1. Before initiating ($t = 0$), the system performs a PU signal test at the suspect sub-carriers. If the PU signal is present, the cognitive system does not send any signal over these sub-carriers. On the contrary, if the PU signal is absent, channel estimation of the cognitive system is carried out, and the payloads are then transmitted over them. If necessary, during payload transmission, PU signal testing may be executed periodically to ensure a quick response to the appearance of the primary network. As shown in Fig. 1, PU signal detection, channel estimation and payload transmission are repeated over and over again (adding PU signal test during payload transmission, if necessary) until the presence of PU signal is detected. Once PU signal is detected either at the system initialization or in the middle of a normal operation, the OFDM system stops transmitting signals over sub-carriers $q \in [q_0, q_1]$. That is, channel estimation and payload transmission are suspended, while the PU signal detection is still performed cyclicly.

The following situation may arise when PU signal monitoring is done concurrently with the transmission of the cognitive system. When a missed detection occurs, the channel estimation will be executed under the presence of the PU signal, resulting in a poor estimation accuracy. These inaccurate channel estimates are subsequently adopted in the next PU signal detection (see (19)–(21) below), which is expected to deteriorate the detection performance. To escape from the vicious cycle, it is required that PU signal detection is carried out in the absence of the cognitive user signal. This can be done by enforcing a "quiet cognitive system" PU signal detection every a given time interval. Or, the channel estimator may calculate the estimation error, e.g. minimum least square (LS) error if an LS estimator is adopted, each time it is executed. If the error is larger than a threshold, a "quiet cognitive system" PU signal detection is initiated.

As described in the previous paragraph, PU signal detection may be executed in both cases of cognitive OFDM being on and off. The received signal at the q -th sub-carrier $Y_q(n)$ is given by (1) with $H_q(n)$ and $S_q(n)$ set to zero when the OFDM system is not transmitting. For $q_0 \leq q \leq q_1$, we build an observation $\bar{\mathbf{Z}}(q)$ from $\{Y_q(n)\}_{n=0}^{N-1}$ such that the PU signal detection is based on the observation along the frequency domain, i.e. $\bar{\mathbf{Z}} = [\bar{Z}(q_0) \bar{Z}(q_0 + 1) \cdots \bar{Z}(q_1)]^T$. We choose

$$\bar{\mathbf{Z}}(q) = \frac{1}{N} \mathbf{Y}_q^\dagger \mathbf{Y}_q, \quad q_0 \leq q \leq q_1, \quad (18)$$

because $\bar{\mathbf{Z}}(q)$ is the periodogram of the received signal at the q -th sub-carrier averaged over N OFDM symbols. It is well known that the periodogram is an estimate of the true spectrum of a signal. Another interpretation of (18) is that the normalized covariance matrix \mathbf{C}_q in the LMP detector of (14) is replaced with the identity matrix due to the unavailability of it. That is, elements of \mathbf{Y}_q are regarded as uncorrelated.

Expanding (18), we obtain

$$\begin{aligned} \bar{\mathbf{Z}}(q) = & \frac{1}{N} \sum_{n=0}^{N-1} (|H_q(n)|^2 + |I_q(n)|^2 + |W_q(n)|^2 + \\ & 2\Re\{H_q(n)S_q(n)I_q^*(n)\} + 2\Re\{H_q(n)S_q(n)W_q^*(n)\} + 2\Re\{I_q(n)W_q^*(n)\}). \end{aligned} \quad (19)$$

Depending on whether the OFDM system is transmitting or not, $H_q(n)$ is either known from channel estimation or equal to zero. We define

$$m(q) := \frac{1}{N} \sum_{n=0}^{N-1} |H_q(n)|^2 + \sigma_W^2, \quad (20)$$

and a new observation is built as

$$Z(q) = \bar{Z}(q) - m(q), \quad (21)$$

which corresponds to subtracting the first and third terms inside the brackets of (19). As the channel experienced by the PU signal is in general frequency-selective, we model the second term in the bracket of (19) by an r -th order polynomial, i.e.

$$\frac{1}{N} \begin{pmatrix} \sum_{n=0}^{N-1} |I_{q_0}(n)|^2 \\ \sum_{n=0}^{N-1} |I_{q_0+1}(n)|^2 \\ \vdots \\ \sum_{n=0}^{N-1} |I_{q_1}(n)|^2 \end{pmatrix} \approx \begin{pmatrix} 1 & 0 & \cdots & 0^r \\ 1 & 1 & \cdots & 1^r \\ \vdots & \vdots & \ddots & \vdots \\ 1 & B_{\text{PU}} - 1 & \cdots & (B_{\text{PU}} - 1)^r \end{pmatrix} \begin{pmatrix} \mu_0 \\ \mu_1 \\ \vdots \\ \mu_r \end{pmatrix} = \mathbf{H}\boldsymbol{\mu}, \quad (22)$$

where we let $r < B_{\text{PU}} - 1$ and the choice of r depends on the selectivity of the channel encountered by the PU signal, μ_i 's are unknowns need to be estimated, and definitions of \mathbf{H} and $\boldsymbol{\mu}$ can be mapped from (22). Moreover, since $S_q(n)$'s are independent for distinct q 's or n 's, and so do $W_q(n)$'s, sums contributing from the three terms at the second line of (19) across $q \in [q_0, q_1]$ can be modeled as zero-mean independent Gaussian random variables for large N .

Let $Z(q)$ be governed by random variable $U_i(u, q)$ under \mathcal{H}_i , where the first argument u , representing a sample point belonging to the sample space, is used to indicate that $U_i(u, q)$ is a random variable. The mean vector of $[U_i(u, q_0) U_i(u, q_0 + 1) \cdots U_i(u, q_1)]^T$ is equal to $\mathbf{0}$ and $\mathbf{H}\boldsymbol{\mu}$ for \mathcal{H}_0 and \mathcal{H}_1 , respectively. Regarding the variance, besides incorporating the three terms in the second line of (19), $U_i(u, q)$ should also include the statistics of the channel estimation error of $H_q(n)$, error between σ_W^2 and $\sum_{n=0}^{N-1} |W_q(n)|^2/N$, and, for \mathcal{H}_1 , the modeling error of $\mathbf{H}\boldsymbol{\mu}$ for the PU signal power. Clearly, distinct magnitudes $|H_q(n)|$ and $|I_q(n)|$ at various q 's result in different variances of $U_i(u, q)$'s; hence, the variances of $U_i(u, q)$'s are better modeled by a polynomial as that in (22). However, this makes the detector design and its analysis difficult. Thus, we model the variances of $U_i(u, q)$'s by an unknown constant σ_i^2 . With above settings, the observation $\mathbf{Z}_{q_0:q_1} = [Z(q_0) Z(q_0 + 1) \cdots Z(q_1)]^T$ is associated with a hypothesis testing of

$$\begin{aligned} \mathcal{H}_0 &: \mathbf{Z}_{q_0:q_1} \sim \mathcal{N}(\mathbf{0}, \sigma_0^2 \mathbf{I}), \\ \mathcal{H}_1 &: \mathbf{Z}_{q_0:q_1} \sim \mathcal{N}(\mathbf{H}\boldsymbol{\mu}, \sigma_1^2 \mathbf{I}), \quad \mathbf{H}\boldsymbol{\mu} \succ \mathbf{0}, \end{aligned} \quad (23)$$

where $\mathbf{H}\boldsymbol{\mu} \succ \mathbf{0}$ means that all elements in $\mathbf{H}\boldsymbol{\mu}$ are greater than 0.

For notational simplicity, in the sequel, subscript of $\mathbf{Z}_{q_0:q_1}$ is omitted if no ambiguity occurs. To perform PU signal detection, GLRT of

$$L_G(\mathbf{Z}) = \frac{p(\mathbf{Z}; \hat{\boldsymbol{\mu}}, \hat{\sigma}_1^2, \mathcal{H}_1)}{p(\mathbf{Z}; \hat{\sigma}_0^2, \mathcal{H}_0)} \quad (24)$$

is employed, where $\hat{\boldsymbol{\mu}}$ and $\hat{\sigma}_i^2$ are ML estimates of $\boldsymbol{\mu}$ and σ_i^2 , respectively. We suppose that the order r of the polynomial used to model the PU signal channel selectivity is suitably chosen; consequently, $\mathbf{H}\hat{\boldsymbol{\mu}} \succ \mathbf{0}$ holds most of the time. Thus, the one-sided test of $\mathbf{H}\boldsymbol{\mu}$ in (23) does not bring serious troubles. Although, when \mathcal{H}_1 is true, $\boldsymbol{\mu}$ and σ_1^2 are both parameterized by the PU signal; however, joint estimate of these two results in a complex detector structure. Thus, $\boldsymbol{\mu}$ and σ_1^2 were deemed to be independent, and they are estimated separately.

It is known that the detector that maximizes (24) is the constant false alarm (CFAR) matched subspace filter [30], given by

$$T_B(\mathbf{Z}) = \frac{B_{\text{PU}} - r - 1}{r + 1} \frac{\mathbf{Z}^T \mathbf{H} (\mathbf{H}^T \mathbf{H})^{-1} \mathbf{H}^T \mathbf{Z}}{\mathbf{Z}^T (\mathbf{I} - \mathbf{H} (\mathbf{H}^T \mathbf{H})^{-1} \mathbf{H}^T) \mathbf{Z}} \sim \begin{cases} F_{r+1, B_{\text{PU}}-r-1}, & \text{under } \mathcal{H}_0, \\ F'_{r+1, B_{\text{PU}}-r-1}(\lambda), & \text{under } \mathcal{H}_1, \end{cases} \quad (25)$$

with

$$\lambda = \frac{1}{\sigma_1^2} \sum_{q=q_0}^{q_1} \sum_{n=0}^{N-1} |I_q(n)|^2, \quad (26)$$

where $F_{a,b}$ denotes an F distribution with a numerator degrees of freedom and b denominator degrees of freedom, and $F'_{a,b}(\lambda)$ denotes a noncentral F distribution with a numerator degrees of freedom, b denominator degrees of freedom and non-centrality parameter λ . This detector tests a signal that is known to lie in a vector space spanned by the columns of \mathbf{H} , but its exact location is unknown because $\boldsymbol{\mu}$ is unknown. Let $Q_{F_{a,b}}(x)$ and $Q_{F'_{a,b}(\lambda)}(x)$ be the right-tail probability evaluated at x for distributions $F_{a,b}$ and $F'_{a,b}(\lambda)$, respectively. Given threshold γ , the false alarm probability of the detector (25) is given by

$$P_{\text{FA}} = Q_{F_{r+1, B_{\text{PU}}-r-1}}(\gamma),$$

which can be used for threshold determination, and the detection probability is

$$P_{\text{D}} = Q_{F'_{r+1, B_{\text{PU}}-r-1}(\lambda)}(\gamma),$$

if an r -th order polynomial is able to model the change of the PU signal powers across sub-carriers q_0 to q_1 .

In getting the detector (25), we assume the PU signal powers over sub-carriers $q \in [q_0, q_1]$ can be modeled by an r -th order polynomial. However, this is not true when either r is not large enough or the channel experienced by the PU signal is severely frequency-selective. Moreover, as mentioned above, characterizing variances of $\{U_i(u, q)\}_{q=q_0}^{q_1}$ for \mathcal{H}_i as a constant is just an approximation. These lead to an inaccurate modeling of (23), and it will of course deteriorate the detector performance. Let us regard the above modeling errors as coming from an interfering signal embedded in $\{Z(q)\}_{q=q_0}^{q_1}$ lying in an unknown subspace. Opportunely, it is shown in [31] that, under a Gaussian environment, the CFAR matched subspace detector of (25) has the robustness for interfering signals that lie in an arbitrary unknown subspace of the observation space. Thus, although some simplifications are made to yield the mean vector and covariance matrices of (23), the proposed detector is robust to them. By robustness, we mean that the false alarm and detection performance suffers less from the presence of unknown subspace interference once a threshold is selected [31].

C. Case C: No Prior Knowledge of PU Signal

In this case, the information of possibly interfered frequency band is unknown. Consequently, the detection algorithm should be involved with a search of the interfered band. Intuitively, given the observation $\mathbf{Z}_{0:Q-1} = [Z(0) Z(1) \cdots Z(Q-1)]^T$, this search is based on the powers at all sub-carriers, and, if the cognitive OFDM system is transmitting signals, a sub-carrier with larger magnitude of frequency response $|H_q(n)|$ tends to be judged as PU signal present. To avoid this problem, the searching of interfered band is executed when the cognitive system is not transmitting signals.

The hypothesis testing associated with Case C is a detection of abrupt changes [32], given as

$$\begin{aligned} \mathcal{H}_0 &: Z(q) \sim U_0(u, q), \quad q \in [0, Q-1], \\ \mathcal{H}_1 &: Z(q) \sim \begin{cases} U_0(u, q), & q \in [0, q_0-1] \cup [q_1+1, Q-1], \\ U_1(u, q), & q \in [q_0, q_1], \end{cases} \end{aligned} \quad (27)$$

where, as specified in the discussion of Case B, $\{U_0(u, q)\}_q$ are white Gaussian with variance σ_0^2 , and $\{U_1(u, q)\}_q$ are independent Gaussian with the means modeled by a polynomial and variance σ_1^2 . All of q_0 , q_1 , σ_0^2 , σ_1^2 and the coefficients of the polynomial are unknown.

We can obtain that the GLRT corresponding to (27) is

$$\max_{q_0, q_1} \frac{(\hat{\sigma}_{0|\mathcal{H}_0}^2)^{Q/2}}{(\hat{\sigma}_{0|\mathcal{H}_1}^2)^{(Q-q_1+q_0-1)/2} (\hat{\sigma}_{1|\mathcal{H}_1}^2)^{(q_1-q_0+1)/2}} \quad (28)$$

where we have

$$\begin{aligned} \hat{\sigma}_{0|\mathcal{H}_0}^2 &:= Q^{-1} \mathbf{Z}_{0:Q-1}^T \mathbf{Z}_{0:Q-1}, \\ \hat{\sigma}_{0|\mathcal{H}_1}^2 &:= (Q - q_1 + q_0 - 1)^{-1} (\mathbf{Z}_{0:q_0-1}^T \mathbf{Z}_{0:q_0-1} + \mathbf{Z}_{q_1+1:Q-1}^T \mathbf{Z}_{q_1+1:Q-1}), \\ \hat{\sigma}_{1|\mathcal{H}_1}^2 &:= (q_1 - q_0 + 1)^{-1} \mathbf{Z}_{q_0:q_1}^T (\mathbf{I} - \mathbf{H}(\mathbf{H}^T \mathbf{H})^{-1} \mathbf{H}^T) \mathbf{Z}_{q_0:q_1}, \end{aligned}$$

denoting estimate of σ_0^2 under \mathcal{H}_0 , estimate of σ_0^2 under \mathcal{H}_1 , and estimate of σ_1^2 under \mathcal{H}_1 , respectively, and \mathbf{H} is given in (22). Defining $f(q_0, q_1)$ as the target to be maximized in (28), we consider the false alarm probability for the detector with threshold γ , i.e.,

$$\begin{aligned} P_{\text{FA}} &= \text{Prob} \left\{ \max_{q_0, q_1} f(q_0, q_1) > \gamma; \mathcal{H}_0 \right\}, \\ &= 1 - \text{Prob} \left\{ f(q_0, q_1) < \gamma, \forall [q_0, q_1] \subset [0, Q-1]; \mathcal{H}_0 \right\}. \end{aligned}$$

Since the random variables governing $f(q_0, q_1)$ for different choices of q_0 and q_1 are not necessarily independent, the determination of P_{FA} and hence the detector threshold for a given $P_{\text{FA}} = \alpha$ becomes intractable.

To conquer this problem, the PU signal detection is decomposed into two steps. In the first step, we search for PU signal's frequency band by observing $\mathbf{Z}_{0:Q-1}$ to get estimates \hat{q}_0 and \hat{q}_1 . In the second step, we assume \hat{q}_0 and \hat{q}_1 obtained in the first step are correct, and we can consequently perform PU signal detection in the same way as that proposed for Case B, where PU signal frequency band is known.

In specific, the first step solves the optimization problem of (28). As the numerator is not a function of q_0 and q_1 , the optimization is equivalent to minimizing the term at the denominator. However, this problem is complex because there are about $Q^2/2$ possible trials for combinations of q_0 and q_1 . To reduce the computational load, we can simplify the optimization problem to one that minimizes the LS error between the observations $Z(q)$'s and the estimated PU signal power, i.e.,

$$\min_{q_0, q_1} \sum_{q \in [0, Q-1] \setminus [q_0, q_1]} Z(q)^2 + \sum_{q \in [q_0, q_1]} \left(Z(q) - \sum_{i=0}^r \hat{\mu}_i (q - q_0)^i \right)^2, \quad (29)$$

where $\{\hat{\mu}_i\}_{i=0}^r$ is the LS solution that minimizes the second term. To compare the ML estimates of q_0 and q_1 and the suboptimal ones, (29) is rewritten in a vector form of

$$\min_{q_0, q_1} \mathbf{Z}_{0:q_0-1}^T \mathbf{Z}_{0:q_0-1} + \mathbf{Z}_{q_1+1:Q-1}^T \mathbf{Z}_{q_1+1:Q-1} + \mathbf{Z}_{q_0:q_1}^T (\mathbf{I} - \mathbf{H}(\mathbf{H}^T \mathbf{H})^{-1} \mathbf{H}^T) \mathbf{Z}_{q_0:q_1}$$

to facilitate examining its relation to the denominator of (28). The solution of (29) can be found by the technique of dynamic programming (DP) [33,34] as follows. Define

$$\delta_0(a, b) := \sum_{q \in [a, b]} Z(q)^2 \quad \text{and} \quad \delta_1(a, b) := \sum_{q \in [a, b]} \left(Z(q) - \sum_{i=0}^r \hat{\mu}_i (q - a)^i \right)^2,$$

where $\{\hat{\mu}_i\}_{i=0}^r$ is the LS solution minimizing $\delta_1(a, b)$. Let

$$e(l) = \min_{0 \leq q_0 \leq l-r} \delta_0(0, q_0 - 1) + \delta_1(q_0, l), \quad r \leq l \leq Q-1, \quad (30)$$

where the constraint $q_0 \leq l - r$ guarantees existence of $\hat{\mu}_i$'s in $\delta_1(q_0, l)$. The optimization problem in (29) is equivalent to

$$\begin{aligned} & \min_{q_0, q_1} \delta_0(0, q_0 - 1) + \delta_1(q_0, q_1) + \delta_0(q_1 + 1, Q-1) \\ &= \min_{q_1} \left\{ \left(\min_{q_0} \delta_0(0, q_0 - 1) + \delta_1(q_0, q_1) \right) + \delta_0(q_1 + 1, Q-1) \right\} \\ &= \min_{r \leq q_1 \leq Q-1} e(q_1) + \delta_0(q_1 + 1, Q-1). \end{aligned} \quad (31)$$

Thus, \hat{q}_1 can be found by searching for q_1 that minimizes (31), and \hat{q}_0 is equal to the value of the argument q_0 in (30) that minimizes $e(\hat{q}_1)$. Note that, the computation of $\delta_1(q_0, l)$'s in solving (30) can be done recursively by sequential LS formulas [35, pp. 242–251].

Suppose that DP yields correct values of q_0 and q_1 . We then employ the detector proposed for Case B to decide whether a PU signal is present in the estimated frequency band. Note that the threshold of the detector output should be a function of \hat{q}_0 and \hat{q}_1 . The performance analysis of the detector is executed as follows. The false alarm probability P_{FA} is

$$\sum_{[a_0, a_1] \subset [0, Q-1]} \text{Prob} \{ \hat{q}_0 = a_0, \hat{q}_1 = a_1; \mathcal{H}_0 \} \cdot \text{Prob} \{ T_B(\mathbf{Z}_{a_0:a_1}) > \gamma_{a_0, a_1}; \mathcal{H}_0 \},$$

where the first probability is the one that DP yields the result of $(\hat{q}_0, \hat{q}_1) = (a_0, a_1)$ under \mathcal{H}_0 , and $T_B(\cdot)$ is given in (25). Given a constraint of $P_{\text{FA}} = \alpha$, we choose the threshold

$$\gamma_{a_0, a_1} = Q_{F_{r+1, a_1 - a_0 - r}}^{-1}(\alpha), \quad [a_0, a_1] \subset [0, Q - 1].$$

Detection occurs when, under \mathcal{H}_1 , DP returns a correct result and the decision statistic is greater than the threshold. When the PU signal power is strong enough such that the frequency band searching is accurate, the detection probability P_D is roughly equal to

$$\begin{aligned} & \text{Prob} \left\{ T_B(\mathbf{Z}_{q_0:q_1}) > Q_{F_{r+1, q_1 - q_0 - r}}^{-1}(\alpha); \mathcal{H}_1 \right\} \\ &= Q_{F'_{r+1, q_1 - q_0 - r}(\lambda)} \left(Q_{F_{r+1, q_1 - q_0 - r}}^{-1}(\alpha) \right), \end{aligned}$$

where λ is given in (26).

IV. SIMULATION RESULTS

Throughout the simulations, the tonal model presented in Paragraph III-A.1 is adopted for the PU signal. The parameters of the PU and cognitive OFDM systems are $T_s = 312.5$ ns, $T_i = 26.6$ μ s, $f_s = 3.1$ GHz, $f_i = 3.36$ GHz, and $Q = 128$. The number of complex sinusoids K contained in the PU signal is adjusted according to the PU signal bandwidth B_{PU} .

In Fig. 2, the receiver operating characteristic (ROC) of several detectors are shown to illustrate the performance of the detector proposed in Case A. The probabilities of miss and false alarm are shown in the vertical and horizontal axes, respectively, for the detection performed at a single sub-carrier. The overall detection performance considering all sub-carriers influenced by the PU signal can be obtained by (6). The observation length N is set to 80 OFDM symbols. During the detection, the cognitive system is not transmitting signals. The curves in the figure are divided into two groups for the power ratio of the PU signal and AWGN being 0 and -2 dB. Within each group, there are four curves. The three solid ones from top to bottom are simulation result of energy detector (test statistic $\mathbf{Y}_q^\dagger \mathbf{Y}_q$), simulation result of LMP detector, and analytical result of estimator-correlator², respectively, and the dashed line is the analytical result of LMP yielded by Gaussian approximation, i.e. $T_A(\mathbf{Y}_q)|_{\mathcal{H}_0}$ is distributed as (16), and $T_A(\mathbf{Y}_q)|_{\mathcal{H}_1}$ is assumed to be Gaussian. It is seen that Gaussian approximation is not accurate under the settings of the simulation environments. Consistently with our intuition, the estimator-correlator has the best performance due to its full knowledge of the observation's PDF, and the energy detector is the worst since the correlation in the PU signal is not exploited.

In Figs. 3 and 4, the simulated ROC curves of the detector proposed in Case B, i.e. (25), are plotted for the environments that the PU signal experiences a channel of eight multipaths with uniform power delay profile and IEEE 802.15.3a ultrawide band (UWB) CM3 model, respectively. In either case, a number of channel realizations are run to obtain an averaged performance. The observation length for detection is 70 OFDM symbols. During detection, the cognitive system is quiet. The average power ratio of the received PU signal and AWGN over the affected sub-carriers is controlled to be 0 dB. The bandwidth of the PU signal B_{PU} and the order r of the polynomial used to model the PU signal powers are indicated on each curve. It is shown that, given the same values of B_{PU} and r , the detector performance shown in Fig. 3 is better than that in Fig. 4, indicating a severe frequency-selective channel of the PU signal deteriorates the performance. This is because the polynomial fails to model the PU signal powers in a hostile channel. Another observation is that, under the same channel type, detection performance improves when B_{PU} increases. While increasing the polynomial order r is not necessarily helpful for detection. This can be explained with the aid of an interpretation for the detector $T_B(\mathbf{Z})$ in (25). Its numerator and denominator can be seen as estimates of the powers of the PU signal and AWGN, respectively [30]. The dimension of the signal subspace is $r + 1$, while it is $B_{\text{PU}} - r - 1$ for the noise subspace. It is required to get a balance between the accuracy of signal and noise estimates by choosing a suitable value of r .

In Fig. 5, the performance of the detector proposed in Case B is demonstrated when the cognitive system is transmitting signals. The power ratio of the cognitive signal to AWGN is set to 8 dB at every sub-carrier. The

²The estimator-correlator is derived from the likelihood ratio test with known received power of the PU signal. The estimator-correlator and its performance can be found in [27, pp.142].

observation length is 70 OFDM symbols. In Fig. 5(a), the average PU signal to noise power ratio versus P_D is plotted when the PU signal experiences a multipath channel with path number equal to eight and uniform power delay profile. The bandwidth B_{PU} , P_{FA} , and polynomial order r are indicated on each curve. Fig. 5(b) shows the same information as Fig. 5(a) with the channel experienced by the PU signal being an IEEE 802.15.3a UWB CM3 channel.

The results of interfered band searching based on (29) of Case C are shown in Fig. 6 for different B_{PU} and observation length N with a *constant* PU signal power over the sub-carriers, i.e. a frequency-flat fading channel. The polynomial order r in (29) is set to 0. A searching is regarded to be a hit if $|q_0 - \hat{q}_0| \leq 1$ and $|q_1 - \hat{q}_1| \leq 1$. It is shown that, with an observation length $N = 70$, the hit percentage approaches 100% at about SNR 1 dB. It can also be seen that the hit percentage is irrelevant to the bandwidth B_{PU} . However, when the PU signal experiences severe frequency-selective fading channel, where there is a notch within the interfered band, our simulation results indicate that the performance of band searching is not as good as that presented in Fig. 6 for an flat-faded PU signal. Examples of channels that result in erroneous estimates of interfered band are shown in Fig. 7, where the channels (sub-carriers 30 to 39) where the PU signal resides are plotted. For each sub-figure, the horizontal and vertical axes are sub-carrier index and squared magnitude of channel frequency response, respectively. In Figs. 7(a) and 7(b), there are spectrum notches within the band; while, in Fig. 7(c), all the sub-carriers suffer from deep fades. In the cases of Figs. 7(a) and 7(b), the estimate $[\hat{q}_0, \hat{q}_1]$ is a subset of the true band $[q_0, q_1]$; in the case of Fig. 7(c), $[\hat{q}_0, \hat{q}_1]$ is not even a subset of $[q_0, q_1]$. Such problem that arises in a severe frequency-selective channel can be conquered by cooperation among cognitive users, as channels from the PU signal source to cognitive users of non-proximity can be regarded as independent.

V. CONCLUSION

In this paper, the problem of PU signal detection in an OFDM based cognitive system is addressed. We categorize the prior knowledge of the PU signal into three cases. In each case, a Neyman-Pearson detector that exploits the prior information is proposed.

In Case A, it is assumed that the PDF's of the received signal under both hypotheses are completely known except for the received power of the PU signal. The frequency band that the PU signal resides is known as well. Since the complexity of finding the estimate of the received PU signal power is high, the use of a GLRT detector is not suggested. In stead, an LMP detector is employed due to the advantages of being optimal for weak PU signal and no need to get the unknown power estimate. Since the covariance matrix involved in an LMP detector is distinct at every sub-carrier, the detection is performed individually at all sub-carriers that the PU signal resides, and the final decision is formed by an OR operation of the results of the individual detections. The simulation result of an LMP detector is compared with an energy detector (information of PU signal covariance matrix not exploited) and estimator-correlator (assuming known PU signal received power). The performance of LMP detector is between the other two.

In Case B, we assume the only PU signal prior information is its residing sub-carriers. The detector proposed for this case exploits the fact that, once the PU signal appears, it interferers a consecutive segment of sub-carriers simultaneously. Measurements obtained at all these sub-carriers are taken as the observation for detection. The associated hypothesis testing is an unknown subspace signal detection in Gaussian noise with unknown variance, where the subspace signal is the PU signal powers across sub-carriers. A CFAR matched subspace detector is the GLRT for the testing, where a polynomial is adopted as the basis of the signal subspace. Although some simplifications are made in formulating the hypotheses, the modeling error can be seen as an interfering signal lying in an arbitrary unknown subspace, and it has been shown that the CFAR matched subspace detector is robust to this kind of unlearned interfering signals under a Gaussian environment.

In Case C, no prior knowledge about the PU signal is available. The detection is involved with a search of interfered sub-carriers. It is shown that the GLRT has high complexity and is difficult to find the output distribution, leading to an undetermined threshold. Thus, the detection is divided into two steps, with the first one searching for the interfered band using an ML criterion and the second deciding whether a PU signal is present in the estimated interfered band. It is easily seen that the second step is just the problem considered in Case B. The first step is further simplified by employing an LS criterion instead of ML, which enables the use of the DP technique to solve the optimization problem. Simulation results show that the searching of interfered band has a very high accuracy if the channel experienced by the PU signal is frequency-flat faded. However, when there is spectrum notch in

the band, the estimation accuracy degrades. It is believed that cooperation among cognitive users is helpful in conquering this problem.

APPENDIX I NORMALIZED COVARIANCE MATRICES OF PU SIGNAL MODELS

A. Tonal PU Signal

Let the cognitive OFDM system have symbol duration T_s , carrier frequency f_s , and its zero-th symbol start at $t = t_0$. We suppose that, at the time the n -th OFDM symbol is received, i.e. $nT_s + t_0 \leq t < (n+1)T_s + t_0$, it is within the span of PU signal's l -th symbol.³ When detecting the n -th OFDM symbol, at the down-converter output of the receiver, the contribution resulting from the PU signal is given by

$$\zeta_l \sum_{k=0}^{K-1} X_{l,k} e^{j2\pi k(t-lT_i)/T_i} e^{j\{2\pi[f_i(t-lT_i) - f_s(t-nT_s-t_0)] + \phi\}}, \quad nT_s + t_0 \leq t < (n+1)T_s + t_0.$$

It is then sampled every $T_d := T_s/Q$ seconds, resulting in Q samples of

$$i_p = \zeta_l \sum_{k=0}^{K-1} X_{l,k} e^{j2\pi(\Delta f + k/T_i)pT_d} e^{j\theta(n,l,k)}, \quad 0 \leq p \leq Q-1, \quad (32)$$

where $\Delta f = f_i - f_s$ and $\theta(n, l, k) = 2\pi[(nT_s + t_0)(f_i + k/T_i) - lf_i T_i] + \phi$. The discrete-time signal $\{i_p\}$ is passed through a Q -point DFT, which gives

$$\begin{aligned} I_q(n) &= \sum_{p=0}^{Q-1} i_p e^{-j2\pi pq/Q} \\ &= \zeta_l \sum_{k=0}^{K-1} X_{l,k} e^{j\theta(n,l,k)} e^{j\pi\beta_{k,q}(Q-1)} \frac{\sin(\pi\beta_{k,q}Q)}{\sin(\pi\beta_{k,q})}, \quad 0 \leq q \leq Q-1, \end{aligned} \quad (33)$$

where $\beta_{k,q} = (\Delta f + k/T_i)T_d - q/Q$. It is seen from (33) that, due to central limit theorem, $\{I_q(n)\}_{n=0}^{N-1}$ can be approximated by a Gaussian random sequence when the number of complex sinusoids K is large enough.

Let us denote by event \mathcal{A} that the n - and m -th OFDM symbols both fall within the span of the l -th PU signal symbol. Clearly, $I_q(n)$ and $I_q(m)$ are zero-mean random variables. Conditioned on event \mathcal{A} , the correlation of $I_q(n)$ and $I_q(m)$ is

$$\mathbb{E}\{I_q(n)I_q^*(m)|\mathcal{A}\} = |\zeta_l|^2 e^{j2\pi(n-m)T_s f_i} \sum_{k=0}^{K-1} e^{j2\pi(n-m)kT_s/T_i} \frac{\sin^2(\pi\beta_{k,q}Q)}{\sin^2(\pi\beta_{k,q})}.$$

On the contrary, if OFDM symbols n and m fall within the spans of distinct symbols of the PU signal, we have

$$\mathbb{E}\{I_q(n)I_q^*(m)|\bar{\mathcal{A}}\} = 0,$$

with $\bar{\mathcal{A}}$ the complement of \mathcal{A} .

Let $\eta := \lfloor T_i/T_s \rfloor$ with $\lfloor x \rfloor$ being the largest integer no greater than x . The probability $\Pr\{\mathcal{A}\}$ of event \mathcal{A} is roughly equal to

$$\Pr\{\mathcal{A}\} = \begin{cases} 1 - \frac{|n-m|}{\eta}, & |n-m| \leq \eta - 1, \\ 0, & \text{otherwise,} \end{cases}$$

where we omit the case the OFDM symbol(s) fall at the border of two PU signal symbols. Thus, the (n, m) -th element of the covariance matrix of $\{I_q(n)\}_{n=0}^{N-1}$ is given by

$$\Pr\{\mathcal{A}\} \cdot \mathbb{E}\{I_q(n)I_q^*(m)|\mathcal{A}\},$$

which leads to the normalized covariance matrix \mathbf{C}_q in (3).

³Although it is possible that an OFDM symbol crosses the boundary of two PU signal symbols, as T_i is in general much larger than T_s , the contribution resulting from this situation is negligible. For instance, if Mobile WiMAX and MB-OFDM-UWB are the sources of the PU signal and the cognitive OFDM system, respectively, the value of T_i/T_s is as large as 329.

B. AR PU Signal

The method to obtain the normalized covariance matrix for AR PU signal basically follows the line presented in [36, pp. 414]. Since \mathbf{I}_q has zero mean, the covariance matrix of \mathbf{I}_q is given by

$$E\{\mathbf{I}_q \mathbf{I}_q^\dagger\} = \mathbf{F}_q \mathbf{R}_i \mathbf{F}_q^\dagger, \quad (34)$$

where \dagger denotes Hermitian transpose, and \mathbf{R}_i is the correlation matrix of the time-domain PU signal \mathbf{i} . From (4), it is readily seen that

$$\begin{pmatrix} 1 & & & & & & \\ & \ddots & & & & & \\ & & 1 & & & & \\ \phi_r & \cdots & \phi_1 & 1 & & & \\ & \phi_r & \cdots & \phi_1 & 1 & & \\ & & \ddots & & & \ddots & \\ & & & \phi_r & \cdots & \phi_1 & 1 \end{pmatrix} \begin{pmatrix} i_0 \\ \vdots \\ i_{r-1} \\ i_r \\ i_{r+1} \\ \vdots \\ i_{QN-1} \end{pmatrix} = \begin{pmatrix} i_0 \\ \vdots \\ i_{r-1} \\ e_r \\ e_{r+1} \\ \vdots \\ e_{QN-1} \end{pmatrix}, \quad (35)$$

which has a notational form of

$$\mathbf{A} \begin{pmatrix} \mathbf{i}_{0:r-1} \\ \mathbf{i}_{r:QN-1} \end{pmatrix} = \begin{pmatrix} \mathbf{i}_{0:r-1} \\ \mathbf{e}_{r:QN-1} \end{pmatrix}, \quad (36)$$

where notation definitions can be easily mapped between (35) and (36). Right-multiplying both sides of (36) by their Hermitian transposes and then taking expectations, we obtain

$$\mathbf{A} \mathbf{R}_i \mathbf{A}^\dagger = \begin{pmatrix} \mathbf{R}_{\mathbf{i}_{0:r-1}} & \mathbf{0} \\ \mathbf{0} & \nu^2 \mathbf{I} \end{pmatrix}, \quad (37)$$

where $\mathbf{R}_{\mathbf{i}_{0:r-1}} = E\{\mathbf{i}_{0:r-1} \mathbf{i}_{0:r-1}^\dagger\}$ is unknown. Since \mathbf{A} is non-singular, we have

$$\mathbf{R}_i^{-1} = \mathbf{A}^\dagger \begin{pmatrix} \mathbf{R}_{\mathbf{i}_{0:r-1}}^{-1} & \mathbf{0} \\ \mathbf{0} & \nu^{-2} \mathbf{I} \end{pmatrix} \mathbf{A}. \quad (38)$$

Partition \mathbf{A} into the following four blocks:

$$\mathbf{A} = \begin{pmatrix} \mathbf{I} & \mathbf{0} \\ \mathbf{A}_{21} & \mathbf{A}_{22} \end{pmatrix}, \quad (39)$$

where the dimensions of \mathbf{A}_{21} and \mathbf{A}_{22} are $(QN-r) \times r$ and $(QN-r) \times (QN-r)$, respectively. Plugging (39) into (38), we can write

$$\mathbf{R}_i^{-1} = \begin{pmatrix} \mathbf{R}_{\mathbf{i}_{0:r-1}}^{-1} + \nu^{-2} \mathbf{A}_{21}^\dagger \mathbf{A}_{21} & \nu^{-2} \mathbf{A}_{21}^\dagger \mathbf{A}_{22} \\ \nu^{-2} \mathbf{A}_{22}^\dagger \mathbf{A}_{21} & \nu^{-2} \mathbf{A}_{22}^\dagger \mathbf{A}_{22} \end{pmatrix}. \quad (40)$$

It is known that the inverse of a nonsingular Toeplitz matrix is persymmetric (i.e., symmetric about the northeast-southwest diagonal) [37]. Since \mathbf{R}_i is Toeplitz, $\mathbf{R}_{\mathbf{i}_{0:r-1}}$ can be determined by comparing $\nu^{-2} \mathbf{A}_{21}^\dagger \mathbf{A}_{21}$ and $\nu^{-2} \mathbf{A}_{22}^\dagger \mathbf{A}_{22}$ in the northwest and southeast blocks of the block matrix in (40). Then, the right-hand-side of (34) can be written as

$$\mathbf{F}_q \mathbf{A}^{-1} \begin{pmatrix} \mathbf{R}_{\mathbf{i}_{0:r-1}} & \mathbf{0} \\ \mathbf{0} & \nu^2 \mathbf{I} \end{pmatrix} (\mathbf{A}^\dagger)^{-1} \mathbf{F}_q^\dagger. \quad (41)$$

Note that since the parameters $\{\phi_j\}_{j=1}^r$ are obtained when the PU signal $\{i_p\}$ has unit power, the matrix given in (41) is the normalized covariance matrix of \mathbf{I}_q .

REFERENCES

- [1] FCC, *Spectrum Policy Task Force Report*, ET Docket No. 02-155, Nov. 02, 2002.
- [2] J. Mitola, "Cognitive radio: making software radio more personal," *IEEE Pers. Commun.*, vol. 6, no. 4, pp. 48–52, 1999.
- [3] J. Mitola, *Cognitive Radio: An Integrated Agent Architecture for Software Defined Radio*, Ph.D. thesis, Royal Institute of Technology (KTH), Sweden, May 2000.
- [4] H. Urkowitz, "Energy detection of unknown deterministic signals," *Proceedings of IEEE*, vol. 55, no. 4, pp. 523–531, 1967.
- [5] V. I. Kostylev, "Energy detection of a signal with random amplitude," in *Proc. IEEE ICC*, Apr. 2002, pp. 1606–1610.
- [6] F. F. Digham, M.-S. Alouini, and M. K. Simon, "On the energy detection of unknown signals over fading channels," in *Proc. IEEE ICC*, May 2003, pp. 3575–3579.
- [7] Marilyn P. Wylie-Green, "Dynamic spectrum sensing by multiband OFDM radio for interference mitigation," in *Proc. IEEE Int. Symp. on New Frontiers in Dynamic Spectrum Access Networks*, Nov. 2005, pp. 619–625.
- [8] A. Ghasemi and E. S. Sousa, "Collaborative spectrum sensing for opportunistic access in fading environments," in *Proc. IEEE Int. Symp. on New Frontiers in Dynamic Spectrum Access Networks*, Nov. 2005, pp. 131–136.
- [9] D. Cabric, A. Tkachenko, and R. W. Brodersen, "Experimental study of spectrum sensing based on energy detection and network cooperation," in *Proc. ACM 1st Int. Workshop on Technology and Policy for Accessing Spectrum*, Aug. 2006.
- [10] S. M. Mishra, A. Sahai, and R. W. Brodersen, "Cooperative sensing among cognitive radios," in *Proc. IEEE Int. Conf. Commun. (ICC) 2006*, June 2006, pp. 1658–1663.
- [11] M. Oner and F. Jondral, "Air interface recognition for a software radio system exploiting cyclostationarity," in *IEEE PIMRC*, Sept. 2004, vol. 3, pp. 1947–1951.
- [12] M. Ghoszi, M. Dohler, F. Marx, and J. Palicot, "Cognitive radio: methods for the detection of free bands," *Comptes Rendus Physique, Elsevier*, vol. 7, pp. 794–804, 2006.
- [13] N. Han, S. Shon, J. H. Chung, and J. M. Kim, "Spectral correlation based signal detection method for spectrum sensing in IEEE 802.22 WRAN systems," in *Proc. Int. Conf. Adv. Commun. Technol.*, Feb. 2006, vol. 3, pp. 1765–1770.
- [14] J. Lunden, V. Koivunen, A. Huttunen, and H. V. Poor, "Spectrum sensing in cognitive radios based on multiple cyclic frequencies," in *Proc. 2nd Int. Conf. Cognitive Radio Oriented Wireless Networks and Communications*, Jul. 31-Aug. 3, 2007.
- [15] E. Visotsky, S. Kuffner, and R. Peterson, "On collaborative detection of TV transmissions in support of dynamic spectrum sensing," in *Proc. IEEE Int. Symp. on New Frontiers in Dynamic Spectrum Access Networks*, Nov. 2005, pp. 338–345.
- [16] T. Weiss, J. Hillenbrand, and F. Jondral, "A diversity approach for the detection of idle spectral resources in spectrum pooling systems," in *Proc. of the 48th Int. Sci. Colloquium*, Sept. 2003.
- [17] G. Ganesan and Y. G. Li, "Agility improvement through cooperation diversity in cognitive radio," in *Proc. IEEE Globecom*, Nov. 2005, vol. 5, pp. 2505–2509.
- [18] G. Ganesan and Y. G. Li, "Cooperative spectrum sensing in cognitive radio: Part I: two user networks," *IEEE Trans. Wireless Commun.*, vol. 6, no. 6, pp. 2204–2213, 2007.
- [19] G. Ganesan and Y. G. Li, "Cooperative spectrum sensing in cognitive radio: Part II: multiuser networks," *IEEE Trans. Wireless Commun.*, vol. 6, no. 6, pp. 2214–2222, 2007.
- [20] M. Gandetto and C. Regazzoni, "Spectrum sensing: a distributed approach for cognitive terminals," *IEEE J. Select. Areas Commun.*, vol. 25, no. 3, pp. 546–557, 2007.
- [21] D. Cabric, S. M. Mishra, and R. W. Brodersen, "Implementation issues in spectrum sensing for cognitive radios," in *Proc. The Thirty-Eighth Asilomar Conference on Signals, Systems and Computers*, Nov. 2004, vol. 1, pp. 772–776.
- [22] S. M. Mishra, S. ten Brink, R. Mahadevappa, and R. W. Brodersen, "Detect and avoid: an ultra-wideband/WiMax coexistence mechanism," *IEEE Communications Magazine*, vol. 45, no. 6, pp. 68–75, 2007.
- [23] I. F. Akyildiz, W.-Y. Lee, M. C. Vuran, and S. Mohanty, "NeXt generation/dynamic spectrum access/cognitive radio wireless networks: A survey," *Computer Networks: The Int. Journal of Computer and Telecommunications Networking*, vol. 50, no. 13, pp. 2127–2159, 2006.
- [24] H. Tang, "Some physical layer issues of wide-band cognitive radio systems," in *Proc. IEEE Int. Symp. on New Frontiers in Dynamic Spectrum Access Networks*, Nov. 2005, pp. 151–159.
- [25] H. L. Van Trees, *Detection, Estimation, and Modulation Theory: Part I. Detection, Estimation, and Linear Modulation Theory*, John Wiley & Sons, Inc., 2001.
- [26] H. Chernoff, "On the distribution of the likelihood ratio," *Ann. Math. Statist.*, vol. 25, no. 3, pp. 573–578, 1954.
- [27] S. M. Kay, *Fundamentals of Statistical Signal Processing: Detection Theory*, vol. 2, Prentice Hall PTR, 1998.
- [28] H. V. Poor, *An Introduction to Signal Detection and Estimation*, Springer-Verlag, New York, 2nd edition, 1994.
- [29] K. S. Miller, *Complex Stochastic Processes*, Addison-Wesley, Reading, Massm, 1974.
- [30] L. L. Scharf and B. Friedlander, "Matched subspace detectors," *IEEE Trans. on Signal Processing*, vol. 42, no. 8, pp. 2146–2157, 1994.
- [31] M. N. Desai and R. S. Mangoubi, "Robust Gaussian and non-Gaussian matched subspace detection," *IEEE Trans. on Signal Processing*, vol. 51, no. 12, pp. 3115–3127, 2003.
- [32] M. Basseville and I. V. Nikiforov, *Detection of Abrupt Changes: Theory and Application*, Prentice Hall, Englewood Cliffs, N. J., 1993.
- [33] C. Myers and L. Rabiner, "A level building dynamic time warping algorithm for connected word recognition," *IEEE Trans. on Signal Processing*, vol. 29, no. 2, pp. 284–297, 1981.
- [34] F. K. Svendsen and F. K. Soong, "On the automatic segmentation of speech signals," in *Proc. 1987 Int. Conf. Acoust., Speech, and Signal Processing, Dallas, TX*, pp. 77–80.
- [35] S. M. Kay, *Fundamentals of Statistical Signal Processing: Estimation Theory*, vol. 1, Prentice Hall PTR, 1993.
- [36] X. Wang and H. V. Poor, *Wireless Communication Systems: Advanced Techniques for Signal Reception*, Prentice Hall PTR, 2004.
- [37] G. H. Golub and C. F. Van Loan, *Matrix Computations*, Johns Hopkins University Press, Baltimore, 2nd edition, 1989.

TABLE I
PRIOR KNOWLEDGE OF THE PU SIGNAL

	<i>Received Power</i>	<i>Signal Model</i>	<i>Gaussian Distribution</i>	<i>Frequency Band</i>
<i>Case A</i>	No	Yes	Yes	Yes
<i>Case B</i>	No	No	Not necessarily	Yes
<i>Case C</i>	No	No	Not necessarily	No

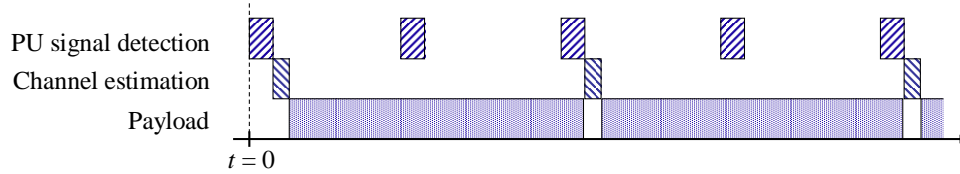


Fig. 1. The signalling of the cognitive OFDM system for the detection algorithm developed in Case B.

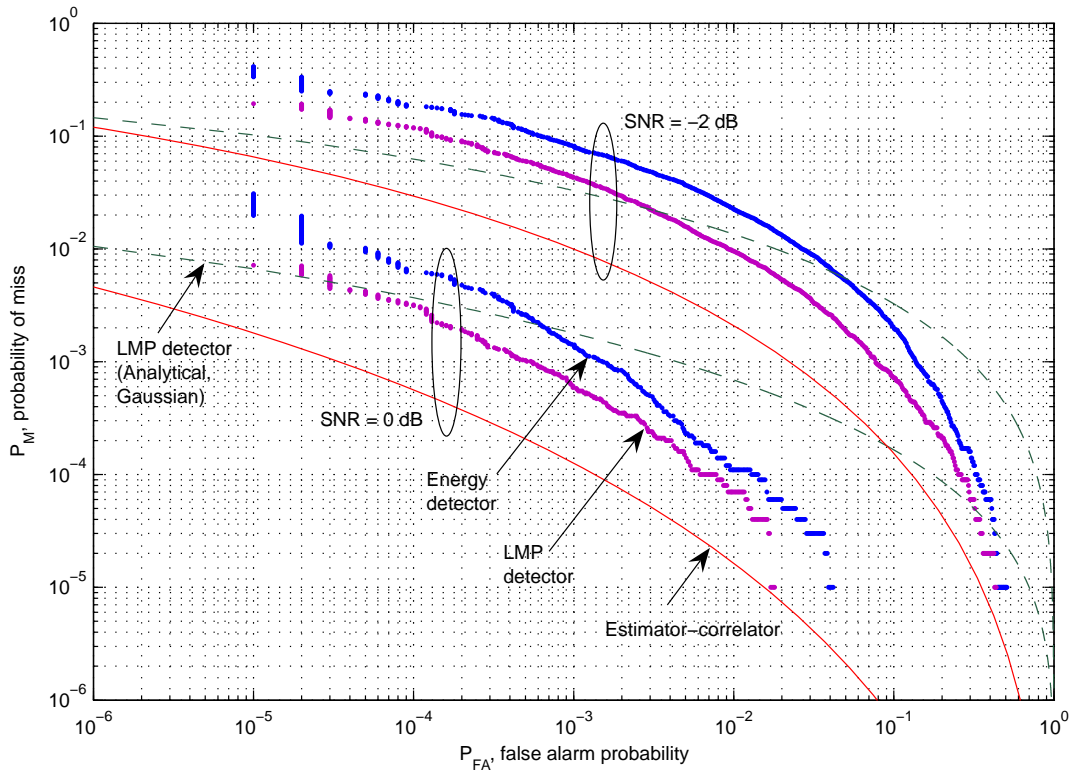


Fig. 2. ROC curves for energy detector, LMP detector and estimator-correlator performed at a single sub-carrier; $Q = 128$, $N = 80$, quiet cognitive system.

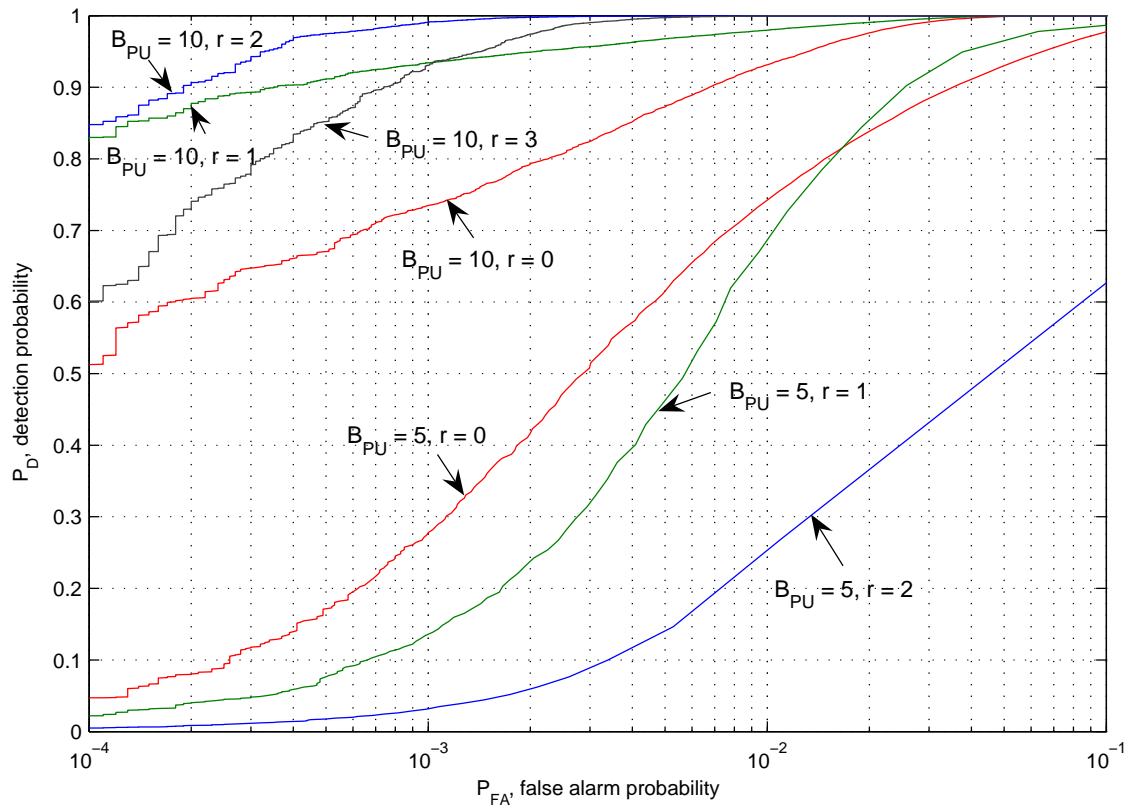


Fig. 3. ROC curves for detector proposed in Case B when the PU signal experiences a multipath channel with path number equal to eight and uniform power delay profile; $Q = 128$, $N = 70$, quiet cognitive system, average PU signal to AWGN power ratio 0 dB.

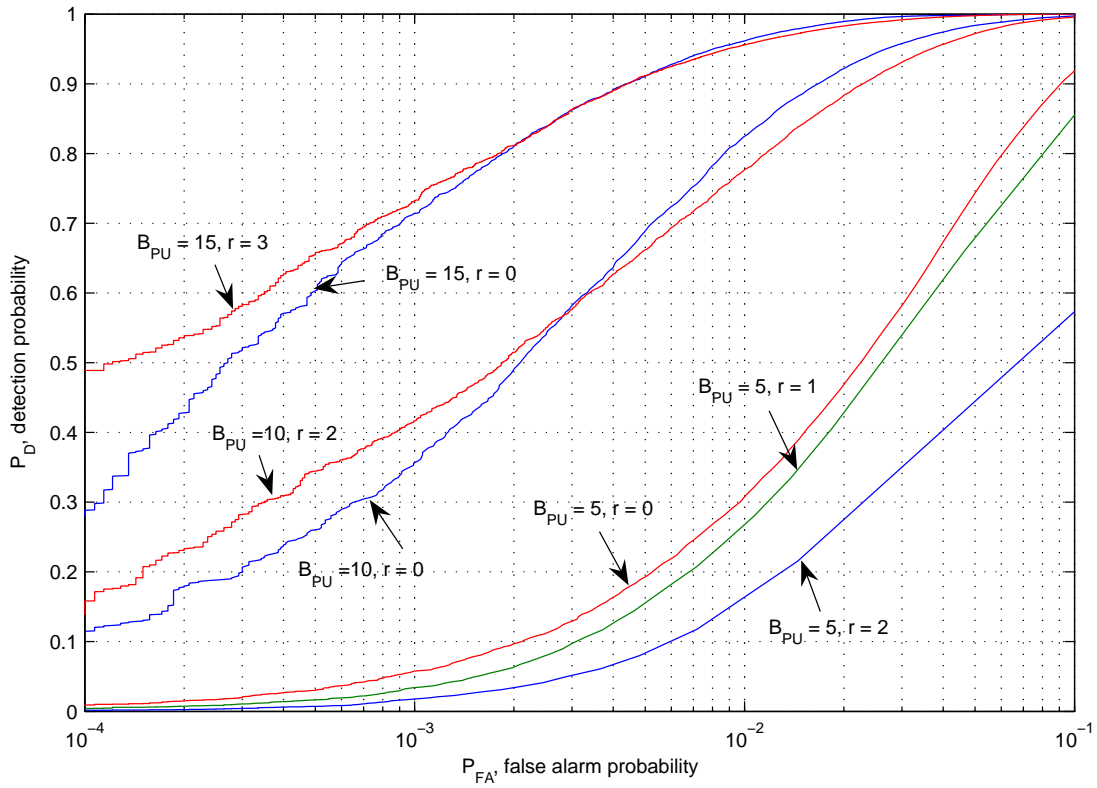
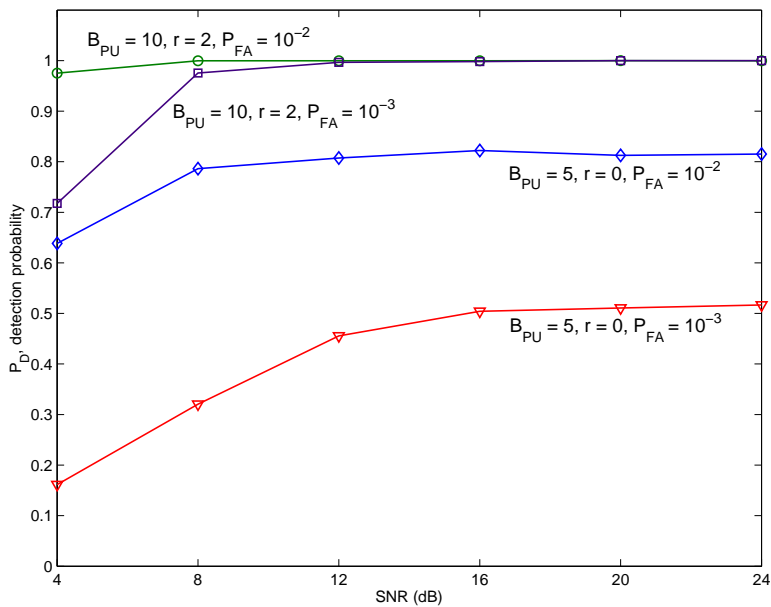
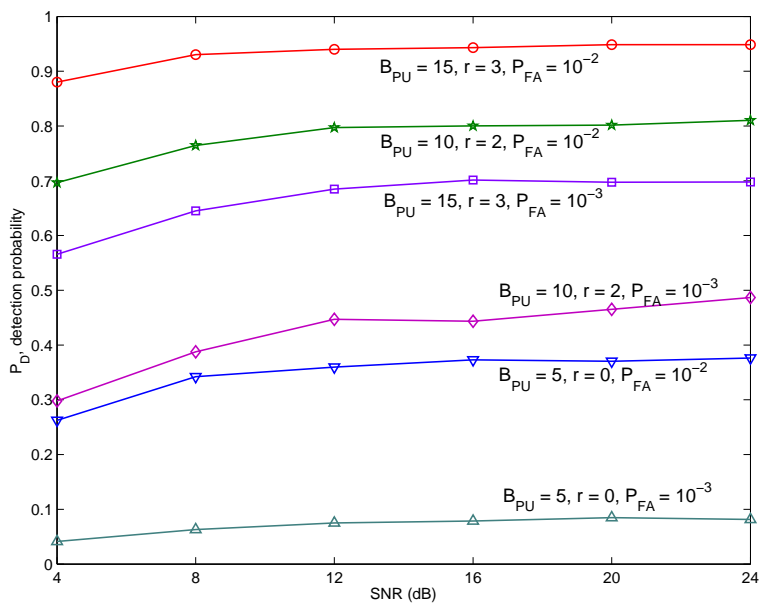


Fig. 4. ROC curves for the detector proposed in Case B when the PU signal experiences an IEEE 802.15.3a UWB CM3 channel; $Q = 128$, $N = 70$, quiet cognitive system, average PU signal to AWGN power ratio 0 dB.



(a)



(b)

Fig. 5. Detection probability versus the power ratio of the PU signal to AWGN for the detector proposed in Case B, when the power ratio of the cognitive signal to AWGN is 8 dB, and the channel experienced by the PU signal is (a) a multipath channel with path number equal to eight and uniform power delay profile, (b) an IEEE 802.15.3a UWB CM3 channel; $Q = 128$, $N = 70$.

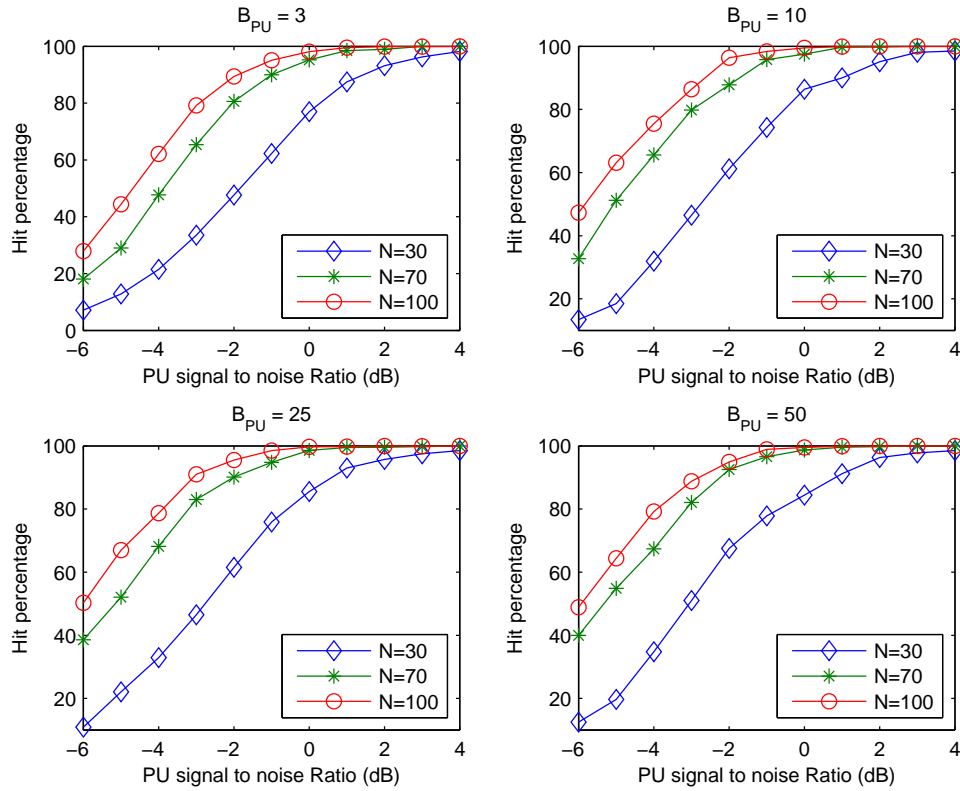


Fig. 6. Hit percentage of the interfered band searching versus the power ratio of PU signal to AWGN for different values of B_{PU} ; constant PU signal power at all sub-carriers, $Q = 128$, quiet cognitive system.

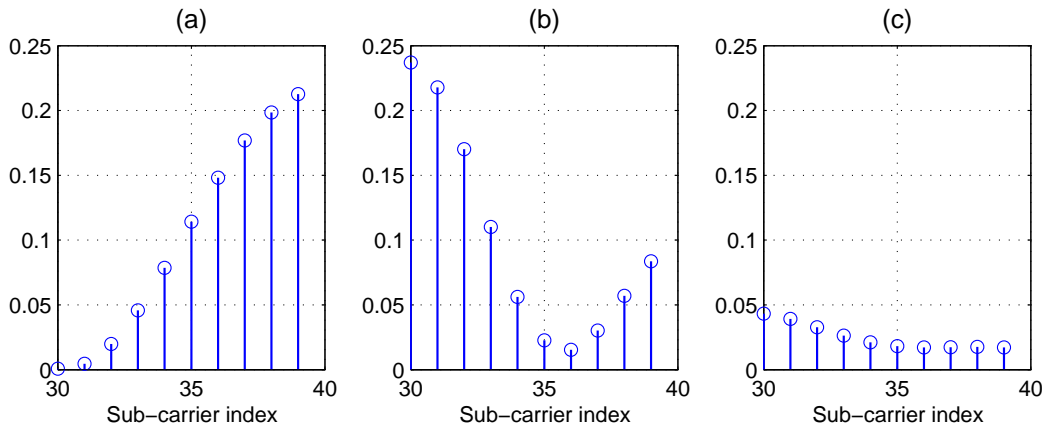


Fig. 7. Examples of frequency-selective fading channels that result in erroneous estimates of interfered band. The vertical axis is the squared magnitude of the channel frequency response.